Journal of Applied Polymer Science

Adsorption of Salicylic Acid in Aqueous Solution by a Water-Compatible Hyper-Cross-Linked Resin Functionalized with Amino-Group

Gu-Qing Xiao,[1] Hua Li,[2] Man-Cai Xu[2]

[1]College of Chemistry and Environmental Engineering, Hunan City University, Yiyang, Hunan 413000, China
[2]College of Chemistry and Chemical Engineering, Hunan Normal University, Changsha, Hunan 410081, China

Correspondence to: G.-Q. Xiao (E-mail: xiaoguqing@yahoo.com.cn)

ABSTRACT: On account of the high toxicity of nitrobenzene, 1,2-dichloroethane was used as solvent. A novel water-compatible hyper-cross-linked resin functionalized with amino-group (denoted as GQ-04) was synthesized to remove salicylic acid (SA) in aqueous solution. The maximum adsorption capacity of SA onto GQ-04 was observed at pH of 1.88. The adsorption capacity increased with the increasing salt concentration. The adsorption kinetic data obeyed the pseudo-second-order rate equation and the adsorption isotherms can be characterized by Freundlich model. The intraparticle diffusion was the main rate-controlling step. The saturated adsorption quantity of SA was up to 119.9 mg·mL-1 according to the dynamic adsorption at 293 K. The resin could be regenerated by the 6 BV mixed solution of 80% ethanol and 0.5 mol/L NaOH. The size matching and hydrogen bonding between GQ-04 and SA and the micropore structure resulted in the larger adsorption capacity in comparison with XAD-4 and H103 resin.
 J. Appl. Polym. Sci. 000: 000–000, 2012

KEYWORDS: synthesis; functionalization of polymers; salicylic ACID; adsorption

Received 5 October 2011; accepted 11 March 2012; published online 00 Month 2012
DOI: 10.1002/app.37686

INTRODUCTION

Salicylic acid (denoted as SA) is one of the most important active principles of many pharmaceutical products. It is widely used as kerotalic, antimicrobial, and antifungal agent.[1] SA is also used as food preservative and plant protection against insects and pathogens.[2] During the manufacturing process of SA, there is a large volume of wastewaters containing SA. The wastewaters present a serious environmental problem because biological degradation of SA occurs too slowly or does not occur at all.[3,4] For some target solutes, it is interesting fact that sorption operations are able to concentrate solutes, especially when these solutes are valuable compounds.

To remove these compounds, many disposal processes are developed and adsorption is proven to be an effective method.[5–7] There are many absorbents in use. Activated carbon is the most widely used for the removal of a variety of organics from waters, but the disadvantage associated with it is the high regeneration cost and the generation of carbons fines because of the brittle nature of carbons. Thus this has simulated research into specialty absorbents using synthetic resins that may facilitate a cheap and effective chemical regeneration process. If chemical modification of the polymeric adsorbents can be performed by introducing some special functional groups onto their skeleton, the obtained polymeric adsorbents will achieve a large adsorption capacity and high adsorption selectivity for some special organic compounds and their potential application in many fields such as wastewater treatment.[8–11]

Nitrobenzene, a carcinogenic pollutant, is widely used as solvent in the production of hyper-cross-linked polymeric adsorbent.[12,13] Even at a low concentration, nitrobenzene may present high risks to ecological and human health because of its toxicity.[14] Therefore, 1,2-dichloroethane was used as solvent in this work.

Carboxyl group in the SA molecular is favorable hydrogen bonding donators. Amino-group is a kind of good hydrogen bonding receptor. The hyper-cross-linked polymeric adsorbents uploaded amino-group on their skeleton can increase the adsorption capacity for SA because of the effect of hydrogen bonding. Aniline can not react with chloromethylated polystyrene by Friedel-Crafts reaction directly because amino-group has the deactivation of benzene ring. GQ-04 functionalized with amino-group can not be synthesized with aniline and chloromethylated polystyrene. A novel water-compatible hyper-cross-linked resin GQ-04 functionalized with amino-group was

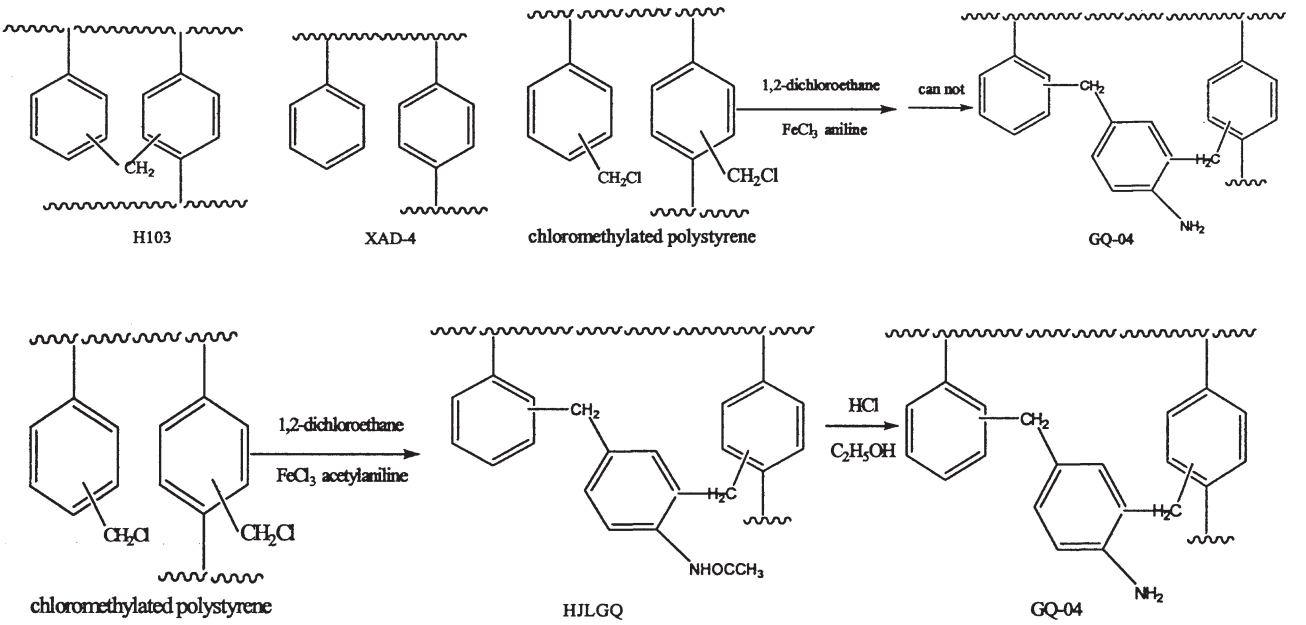

Figure 1. Scheme of the resins.

synthesized as described in Figure 1. The objective of this work was to study the adsorption performances for SA onto GQ-04.

EXPERIMENTAL

Materials

Macroporous low cross-linked chloromethylated polystyrene beads were provided by Langfang Chemical (Hebei province, P.R. China, the crosslinking degree: 6%, the chlorine content: 17.3%). The Amberlite XAD-4 resin was purchased from Rohm & Haas Company (Philadelphia, PA). H103 resin was purchased from the chemical plant of NanKai University (Tianjin city, China). SA, ferric chloride, dichloroethane, and acetylaniline were analytical reagents.

Synthesis of GQ-04

As described in Figure 1, 30 g of chloromethylated polystyrene beads was swollen by 300 ml of 1,2-dichloroethane overnight at the temperature of 298 K. Under mechanical stirring, 2.4 g acetylaniline was added, and then 7.5 g of newly treated ferric chloride was added into the flask as quickly as possible. The reaction mixture was further stirred at 353 K for 10 h. Finally, the mixture was poured into an ethanol bath containing 1% of hydrochloric acid (w/w). The polymer bead was filtered and extracted with ethanol in a Soxhlet apparatus for 10 h and then dried under vacuum at 323 K for 10 h. The hyper-cross-linked resin was hydrolyzed at 350 K for 12 h in the solution of surplus hydrochloric acid and ethanol, and hence GQ-04 was achieved.

Characterization of the Adsorbents

The infrared (IR) spectra of all samples were obtained on a Nicolet 510P Fourier transformed IR instrument by KBr disks. The specific surface area was determined via the N_2 adsorption-desorption isotherms using an ASAP 2010 surface area measurement instrument.

Kinetic Adsorption

The kinetic studies were performed at 293K. 2.001 g wet GQ-04 was added to 1000 ml of 0.704 mg/mL SA solution. The mixture was shaken mechanically at 200 rpm. Supernatant solution at certain time interval was taken to monitor the concentration of SA by ultraviolet spectrometry at 296.1 nm.

Static Adsorption Equilibrium

Equilibrium adsorption of SA onto GQ-04 was performed at 293, 298, 303, and 308 K, respectively. 0.200 g GQ-04 and 50 ml SA solution of different known initial concentration, C_0 (mg/L), were added into cone-shaped flasks. The flasks were shaken at a presettled temperature until the adsorption equilibrium was reached, and the equilibrium concentration of SA, C_e (mg/L), was determined by ultraviolet spectrometry. The

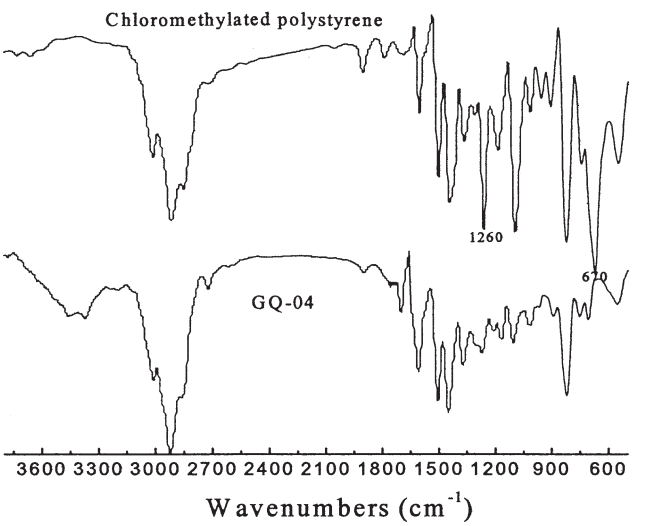

Figure 2. IR spectra of resins.

Table I. The Values of BET Surface, Pore Volume, and Pore Diameter of the Resins

	BET surface (m^2/g)	Micropore surface (m^2/g)	Pore volume (cm^3/g)	Pore diameter (nm)	Polarity
Chloromethylated polystyrene	24.76	3.84	0.061	9.93	-
HJLGQ	734.19	419.15	0.53	2.88	-
GQ-04	770.69	444.57	0.55	2.87	Weak polar
XAD-4	950.95	46.02	1.25	5.25	Nonpolar
H103	1069.47	458.65	0.95	3.55	Nonpolar

equilibrium adsorption capacity of SA, q_e (mg/g), was calculated as $q_e = (C_0\text{-}C_e)V/W$. V was the volume of the aqueous solution (L), and W was the weight of GQ-04 (g).

Dynamic Adsorption and Desorption

A 10 mL aliquot of wet GQ-04 were packed into a glass column (inner diameter 10 mm) and prewashed with 10 mL deionized water. The column kept undisturbed. A sample of 0.8 mg/mL SA was passed through the column at a flow rate of 2.8 BV/h. The adsorption process was continued until all the resin was saturated by SA. After the adsorbent in the fixed bed was saturated by SA, the mixed solution of 80% C_2H_5OH and 0.5 mol/L NaOH was used to regenerate GQ-04. The flow rate of the mixed solution was kept at 1.5 BV/h.

RESULTS AND DISCUSSION

Characterization of the Adsorbents

The IR spectrum (presented in Figure 2.) of GQ-04, two strong characteristic bands related to the —CH_2Cl groups at 1260 and 670 cm^{-1} are weakened greatly, whereas another strong vibration with frequencies at 3100–3700 cm^{-1} is presented, and the band at 3100–3700 cm^{-1} is concerned with the characteristic adsorption peaks of the N—H, indicating that aniline has been attached to the framework of GQ-04.

The BET surface area and pore volume of GQ-04 (presented in Table I) are measured to be 770.69 m^2/g and 0.55 cm^3/g, respectively, much higher than those of the chloromethylated polystyrene, much lower than the corresponding ones of XAD-4 and H103. The results of the pore distribution of GQ-04, XAD-4, and H103 are shown in Figure 3. The pore distribution of the three resins is distinguishing. The pore distribution indicates that GQ-04 and H103 contain some macropores. A good deal of micropores is present in GQ-04 and H103 resin whereas very few micropores are for XAD-4. Moreover, the mesopores in the range of 2–50 nm are predominant for GQ-04 and H103, whereas the mesopores of 2–18 nm play an important role for XAD-4. Compared with GQ-04, the values of BET surface, pore volume, and pore diameter of HJLGQ are no obvious different, revealing that hydrolysis reaction does not induce great change for the pore of the two kinds of resin.

Adsorption Isotherms

Figure 4 presents the adsorption isotherms of SA onto GQ-04 in aqueous solution at 293, 298, 303, and 308 K, respectively. It is clear that low temperature is favorable for the adsorption, indicating an exothermic process.[15] In this study, the equilibrium data are fitted to the Freundlich isotherm $Q = k_F C^{1/n}$. K_F and n are the characteristic constants. The values of K_F and n, and the correlation coefficients R are shown in Table II. It can be seen that all the experimental adsorption isotherms coincide with the Freundlich model because all the correlation coefficients are higher than 0.99. As known to us, K_F is considered to be an indicator of the adsorption capacity. The values of K_F decrease with the increase of temperature, consistent with the fact that low temperature is favorable for the adsorption.

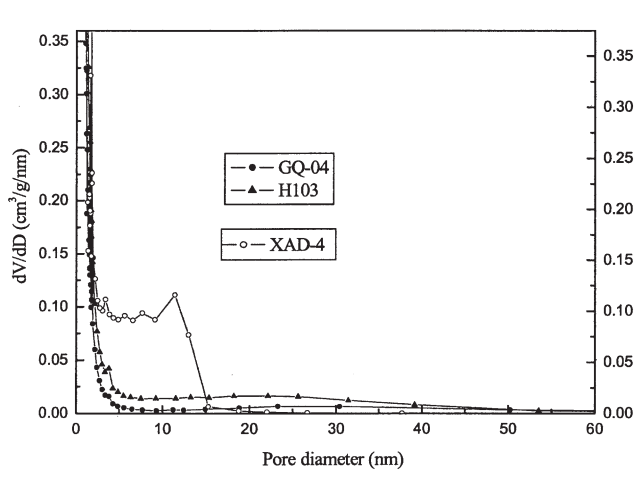

Figure 3. The pore distribution of the resins.

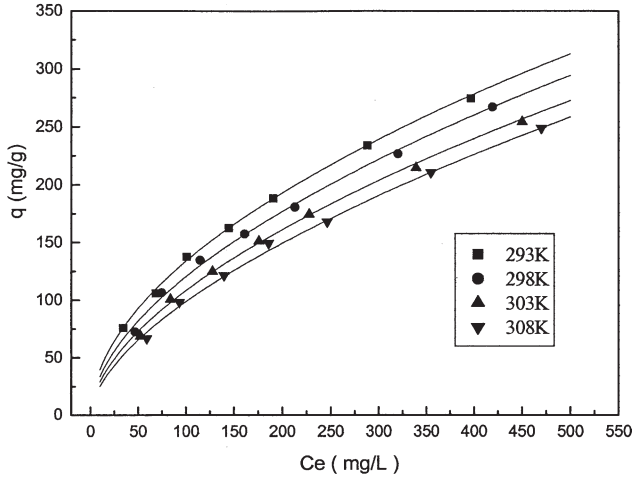

Figure 4. Adsorption isotherms of SA onto GQ-04.

Table II. Fitting Parameters of the Freundlich Isotherm for GQ-04

	Freundlich isotherm $Q = k_F C^{1/n}$		
$T(K)$	K_F	n	R
293	11.517	1.882	0.9993
298	8.581	1.752	0.9956
303	6.990	1.692	0.9972
308	5.705	1.621	0.9965

Effect of Salt Concentration on the Adsorption Capacity of GQ-04

Inorganic salts such as NaCl and Na_2SO_4 are often coexistent in industrial wastewater with a comparatively high concentration, and hence the effect of NaCl (as the model of inorganic salt) on the adsorption capacity of GQ-04 is determined. The result is shown in Figure 5. The adsorption capacity of SA onto GQ-04 increases with the increasing salt concentration, which may be from the so called "salting-out" effect.[16]

Effect of Solution pH on the Adsorption Capacity of GQ-04

The solution pH is one of the most important factors influencing the adsorption of SA onto GQ-04. The adsorption capacity of SA onto GQ-04 at different pH values is shown in Figure 6. Proportion of SA molecular state is calculated from the value of pka_1 (2.98) of SA.

The adsorption is sensitive to the solution pH. It is seen that the maximum adsorption capacity is observed at pH of 1.88 and lower or higher pH is unfavorable for the adsorption. Amino-group on resin will accept a proton, and therefore, will carry the decrease of adsorption capacity for SA at pH less than 1.88. It can be seen that the adsorption capacity of SA onto GQ-04 decreased at pH greater than 1.88. It may be the reason that the structure of SA changes at different pH values of the solution because of the hydroxyl group and carboxyl group in the SA molecular. In the acidic, SA is represented as an SA molecule. The adsorption capacity of SA decreases gradually with the increase of the solution pH because SA is ionized.

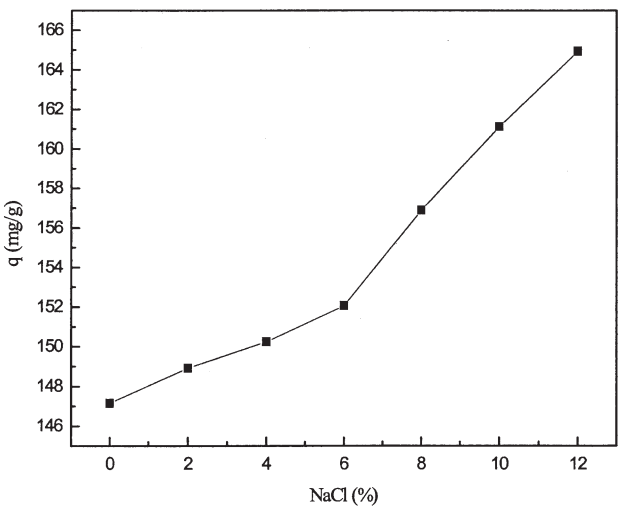

Figure 5. Effect of salt concentration on the adsorption.

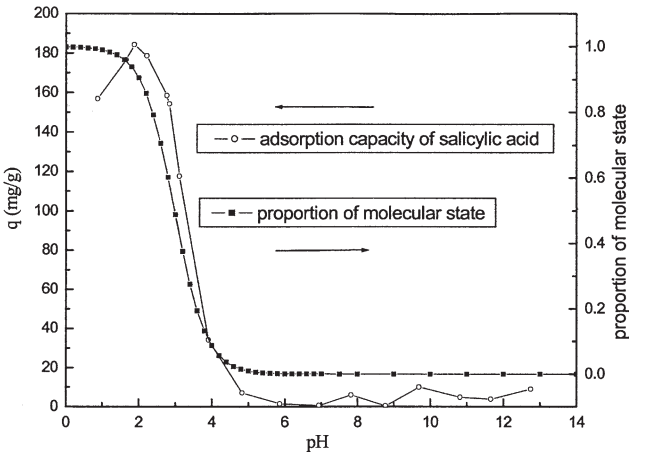

Figure 6. Effect of solution pH on the adsorption.

Adsorption Kinetics

The pseudo-second-order equation[15–17] $\frac{1}{q_e - q_t} = \frac{1}{q_e} + k_2 t$ is used to fit the adsorption kinetic data. Here q_t (mg/g) is the capacity of SA at the contact time t (min), the equilibrium capacity of SA q_e (mg/g), and k_2 (min^{-1}) is the pseudo-second-order rate constants, respectively. The fitted adsorption kinetic curves by the pseudo-second-order rate equation are shown in Figure 7. The fitted results indicate the corresponding rate constants $k_2 = 3.44 \times 10^{-5}$ $g \cdot mg^{-1} \cdot min^{-1}$. As shown in Figure 7, the pseudo-second-order rate equation can characterize the adsorption well because of the correlation coefficients $R = 0.997$.

The intraparticle diffusion model[17] $q_t = k_i t^{0.5}$ is used to fit the adsorption kinetic data. Here k_i is the diffusion rate parameter {[(mg/g)/(min)$^{-1/2}$]}. The k_i is calculated to be 17.51 (mg/g·$min^{0.5}$), the correlation coefficients $R = 0.997$. As shown in Figure 8, plots of q_t versus $t^{1/2}$ for the beginning adsorption process result in a linear relationship, and the straight line does not pass through the origin, indicating that the intraparticle diffusion is the main rate-limiting step for the adsorption.[17] Adsorption rate was also affected by the impact of film diffusion.[17]

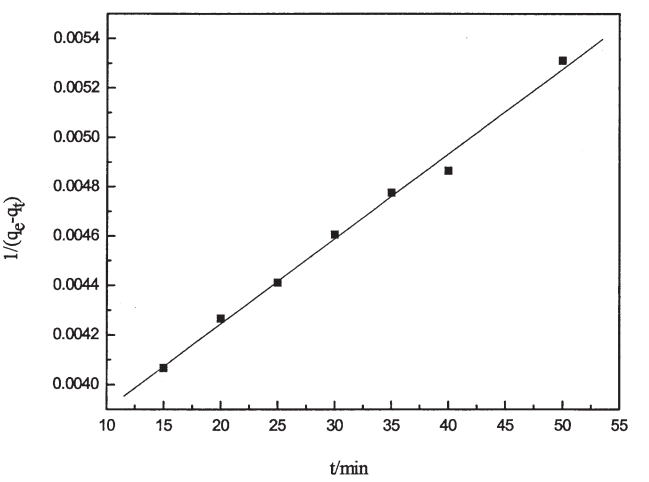

Figure 7. The Lagergren second order adsorption kinetics equation of SA onto GQ-04.

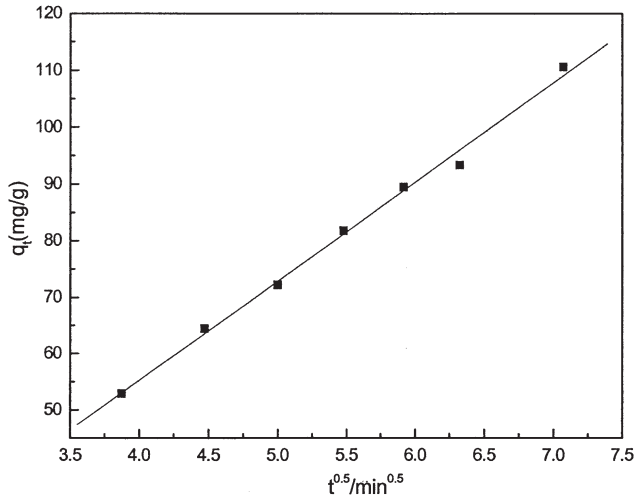

Figure 8. The rate of intraparticle diffusion of SA onto GQ-04.

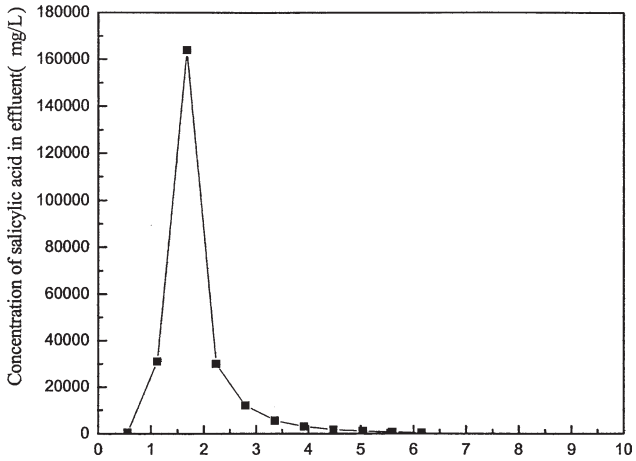

Figure 10. Fluidizing desorption curve of the SA.

Dynamic Adsorption and Desorption

The results of dynamic adsorption experiments for SA under the condition of 293 K are shown in Figure 9. The outlet SA concentration reaches 1% of the feed SA concentration after eluting 83.9 bed volumes. The saturated adsorption quantity of SA is up to 119.9 mg·mL^{-1} when the outlet SA concentration reaches 100% of the feed SA concentration. The results of SA elution experiments are shown in Figure 10. GQ-04 can be regenerated by the 6 BV mixed solution 80% C_2H_5OH and 0.5 mol/L NaOH.

Adsorption Mechanisms

The adsorption isotherms of SA onto GQ-04, XAD-4, and H103 resin are examined at 298 K, and the results are shown in Figure 11. It is clear that the adsorption capacity of SA onto GQ-04 resin is enhanced in comparison with XAD-4 and H103 resin.

The BET surface area of XAD-4 is larger than the corresponding one of GQ-04, whereas the adsorption capacity of SA onto XAD-4 is much smaller than GQ-04. That is, the BET surface area does not play an important role. This different adsorption capability may be explained. It was found that the optimum ratio of the pore diameter of the adsorbent to the molecular size of the adsorbate was 3–6 for polymeric adsorbents.[15] The molecular size of SA is calculated to be 0.704 nm × 0.459.[18] The average pore diameter of GQ-04 is measured to be 2.87 nm, which is helpful for the adsorption, whereas the average pore diameter of XAD-4 is 5.25 nm, which is too big for the adsorption of SA and affects the adsorption in a negative way. From another opinion, a good deal of micropores in GQ-04 can be helpful for the adsorption capability of SA, whereas very few micropores are for XAD-4.

As shown in Figure 3, both GQ-04 and H103 owns a good deal of micropores. Although H103 has a higher surface area than GQ-04, it has a smaller adsorption capacity than GQ-04. This can be explained from the hydrogen bonding.

Because aniline is uploaded on GQ-04 resin, it is used to simulate GQ-04 resin to be calculated with density functional

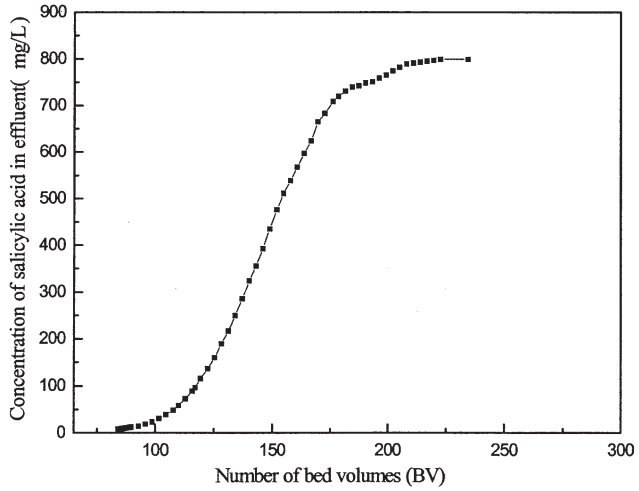

Figure 9. Fluidizing adsorption curve of the SA.

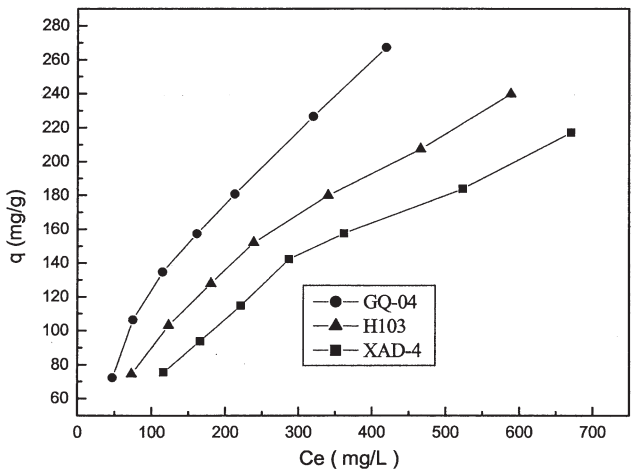

Figure 11. Comparison of the adsorption property of SA onto the resins.

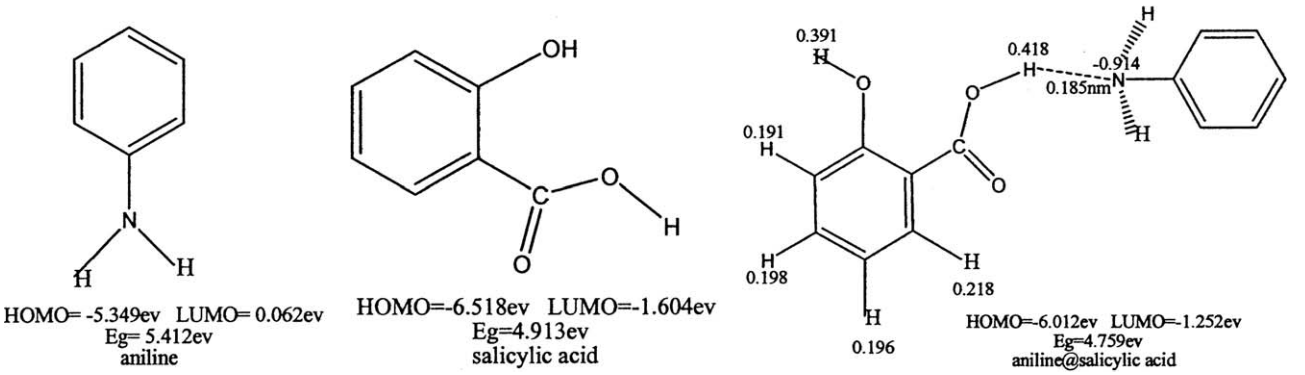

Figure 12. Some main atom Mulliken charge, bond length, and the energy of HOMO and LUMO.

theory (DFT) method at RB3LYP/6-311G(d) level. DFT has been performed on the aniline, SA, and their complex (aniline@SA). The results of some main atom Mulliken charge, bond length, as well as the energy of HOMO and LUMO are shown in Figure 12. The length of N atom of aniline and H atom of SA is 0.185 nm, shorter than the sum of van der Waals radius of H (0.120 nm) and N (0.155 nm),[19] longer than the bond length of N—H, which is the cause that the hydrogen bonding is formed between N atom of aniline and H atom of SA. Moreover, Mulliken charge of H atom onto carboxyl group is 0.418, which is higher than any other H atom of SA, and Mulliken charge of N atom of aniline is -0.914, hence N atom of aniline can form strong hydrogen bonding with H atom of SA. Furthermore, after hydrogen bonding is formed, both the highest occupation orbital energy E_{HOMO} and the lowest empty orbital energy E_{LUMO} of the complex (aniline@SA) are lower than those of aniline, and the energy gap in E_{HOMO}-E_{LUMO} is lower than any of aniline and SA. Hydrogen bonding can improve the ability of adsorption for SA onto GQ-04 resin, whereas H103 is nonpolar.

The size matching of the pore diameter of GQ-04 and the molecular size of SA, hydrogen bonding between GQ-04 and SA, and the micropore structure result in the larger adsorption capacity in comparison with XAD-4 and H103 resin.

CONCLUSIONS

The adsorption property of SA onto GQ-04 was superior to XAD-4 and H103 obviously. The saturated adsorption quantity of SA was up to 119.9 $mg \cdot mL^{-1}$ according to the dynamic adsorption at 293 K. The resin could be regenerated by the 6 BV mixed solution of 80% ethanol and 0.5 mol/L NaOH. GQ-04 displays an excellent adsorption behavior, implying GQ-04 can be looked on as a potential adsorbent for removal of SA in aqueous solution.

ACKNOWLEDGMENTS

We gratefully acknowledge generous support provided by the Nature Science Foundation of science and technology department of Hunan Province (Grant No.2011SK3126) P. R. China.

REFERENCES

1. Otero, M.; Grande, C. A.; Rodrigues, A. E. *React. Funct. Polym.* **2004,** *60*, 203.
2. Otero, M.; Zabkova, M.; Rodrigues, A. E. *Sep. Purif. Technol.* **2005,** *45*, 86.
3. Boussetta, S.; Branger, C.; Margaillan, A.; Boudenne, J. L.; Coulomb, B. *React. Funct. Polym.* **2008,** *68*, 775.
4. Davis, D. P.; Daston, G. P.; Odio, M. R.; Kraus, A.C.*Toxicol. Lett.* **1996,** *84*, 135.
5. Tao, W. H.; Li, A. M.; Long, C.; Qian, H. M.; Xu, D. J.; Chen J. J. *Hazard. Mater.* **2010,** *175*, 111.
6. Anirudhan, T. S.; Rijith, S.; Suchithra, P. S. *J. Appl. Polym. Sci.* **2010,** *115*, 2069.
7. Li, J. Z.; Yao, K. D. *J. Appl. Polym. Sci.* **2005,** *96*, 841.
8. Yuan, S. G.; Zhang, S. H.; Zou, W. H.; Zhou, Y. H.; Zhou, X. H. *Chin. Chem. Lett.* **2008,** *19*, 611.
9. He, C. L.; Huang, K. L.; Huang, J. H. *J. Colloid Interface Sci.* **2010,** *342*,462.
10. Fontanals, N.; Galia, M.; Cormack, P. A.; Marce, R. M. *J. Chromatogr. A* **2005,** *1075*, 51.
11. Hradil, J.; Sysel, P.; Kovarova, J.; Kotek J. *React. Funct. Polym.* **2007,** *67*, 432.
12. Zheng, K.; Pan, B. C.; Zhang, Q. J.; Zhang, W. M.; Pan, B. J.; Han, Y. H.; Zhang, Q. R.; Wei, D.; Xu, Z. W.; Zhang, Q. X. *Sep. Purif. Technol.* **2007,** *57*, 250.
13. Li, A. M.; Zhang, Q. X.; Zhang, G. C.; Chen, J. L.; Fei, Z. H.; Liu, F. Q. *Chemosphere* **2002,** *47*, 981.
14. Anotai, J.; Sakulkittimasak, P.; Boonrattanakij, N.; Lu, M. C. *J. Hazard. Mater.* **2009,** *165*, 874.
15. Huang, J. H.; Huang, K. L.; Liu, S. Q. *J. Hazard. Mater.* **2009,** *162*, 771.
16. Sun, Q. Y.; Yang, L. Z. *Water. Res.* **2003,** *37*, 1535.
17. Huang, J. H.; Yan, C.; Huang, K. L. *J. Colloid Interface Sci.* **2009,** *332*, 60.
18. Frisch, M. J. Gaussian 03, Gauss View B.05; Gaussian, Inc.: Pittsburgh, PA, **2003.**
19. Hu, S. Z.; Xie, Z. X.; Zhou, Z. H. *Acta Phys. Chim. Sin.* **2010,** *26*, 1795.